PERGAMON

Electrochimica Acta 44 (1999) 4763–4771

ELECTROCHIMICA Acta

www.elsevier.nl/locate/electacta

Characteristics of the polyaniline anodic pre-peak

Huyen N. Dinh, Viola I. Birss *

Department of Chemistry, University of Calgary, 2500 University Drive N.W., Calgary, Alta., Canada T2N 1N4

Received 22 February 1999; received in revised form 2 June 1999

Abstract

A detailed study of the origin and meaning of the anodic pre-peak, A_0, was carried out for polyaniline (PANI) films, which were electrochemically grown using the potential sweep method to two different upper potential limits (Type I and Type II films) on Au, Pt and GC electrodes. The observed presence of a matching cathodic peak, C_0, for slowly grown Type I films, and the absence of the A_0 pre-peak for rapidly formed Type II films, suggest that the pre-peak arises from the oxidation of particular PANI sites within these films, likely located near the underlying substrate. Time of cycling over the A_0/C_0 potential range (0 and 0.3 V) and/or holding of the potential in the reduced film state causes the A_0 peak potential to shift. Simultaneous cyclic voltammetry, quartz crystal microbalance and ellipsometry measurements indicate that the positive movement of the A_0 potential is related to film swelling. Long times of cycling between 0 and 0.6 V appear to cause the Type I film to anneal, resulting in a more compact PANI film, and a negative shift of the pre-peak. The pre-peak, therefore, appears to be a barometer of film water and/or solution anion content.

Keywords: Polyaniline; Pre-peak; Film annealing; Cyclic voltammetry; Quartz crystal microbalance

1. Introduction

In cyclic voltammetry (CV) experiments, the electrochemical conversion from the reduced to oxidized form of polyaniline (PANI) films is sometimes preceded by a small anodic pre-peak [1,2]. This pre-peak has been seen in published PANI CVs in HCl and H_2SO_4 solutions [1–3]. However, little detailed attention has been paid to its interpretation to date.

Gottesfeld et al. have suggested that the pre-peak (A_0) is caused by the change in bulk PANI film resistivity as it switches from the insulating to the conducting form [3,4]. According to this theory, the anodic pre-peak results from the initial spread of electronic conductivity through a network of dense, non-conducting fibers within the PANI film. This small amount of anodic charge injection is then suggested to significantly increase the electronic conductivity of the film, thus yielding the pre-peak [3]. Gottesfeld et al. suggested that starting the positive scan at a relatively negative potential, e.g. an E_- of 0 V, and/or increasing the time spent at E_-, would serve to reduce the PANI film more fully [3]. The resulting further increase in film resistivity would delay the onset of film oxidation, causing a positive shift of the pre-peak in the first anodic scan [3]. In subsequent scans, the pre-peak was predicted to broaden and shift negatively to a steady state potential [3], as seen experimentally.

Kalaji et al. [5] have carried out holding experiments at comparatively negative potentials near 0 V versus SHE, but perhaps because only a thin PANI film (36 nm) was studied, no pre-peak was observed. Instead, time spent at 0 V resulted in the principal anodic peak (A_1) being somewhat larger and shifted positively by ca. 100 mV versus its steady-state position in multi-cycling experiments. Also, the charge passed in the first oxida-

* Corresponding author. Tel.: +1-403-2206432; fax: +1-403-2899488.

E-mail address: birss@ucalgary.ca (V.I. Birss)

0013-4686/99/$ - see front matter
PII: S0013-4686(99)00224-8

tion cycle after holding at E_- was not fully recovered in the subsequent cathodic sweep, i.e. the PANI film was not fully reduced. Subsequent multi-cycle scans did not show a positive shift of A_1 and the anodic and cathodic charges were the same. Like Gottesfeld et al. [3], the authors [5] explained that, by spending time at negative potentials, PANI films become completely reduced, and added that the rate of oxidation is slower in this case than when the film is only partially reduced [5]. However, they did not attempt to explain the origin of the A_0 pre-peak using this argument [5].

A similar anodic pre-peak is seen during the oxidation of non-conducting Ir(III) oxide to the conducting Ir(IV) state. It was also explained as being due to the switch of the film conductivity [3]. However, it was later reported that [6–8], when Ir oxide films are transferred from acidic solutions, where the pre-peak is seen, to basic solutions, the pre-peak is completely absent. As Ir oxide films are still fully electrochromic and conductivity switching in alkaline solutions, it was concluded [6–8] that the pre-peak must arise from additional factors than just the increase in film conductivity during the anodic sweep.

In the present work, the origin of the anodic pre-peak, A_0, was explored in detail by studying PANI films grown slowly in 1 M H_2SO_4 by multi-cycling to $E_+ = 1$ V versus RHE (Type I PANI) and those grown much more rapidly to $E_+ = 1.7$ V versus RHE (Type II PANI), on Au, Pt and GC electrodes. Concurrent CV and quartz crystal microbalance (QCMB) measurements were carried out to determine the mass change associated with the pre-peak reaction. Ellipsometric measurements were also carried out to monitor the optical properties of PANI films in the potential range of the A_0 peak, in particular.

2. Experimental

2.1. Equipment

Cyclic voltammetry (CV) was performed using EG and G PARC 173/175 instrumentation, while the quartz crystal microbalance (QCMB) experiments were carried out using a home-made, Pierce-type oscillator, connected to a Philips PM 6654C programmable high resolution frequency counter. A Gaertner L116C ellipsometor was used in the monochromatic mode (633 nm) to monitor the optical properties of the PANI film at 0 V versus RHE. The details of the instrumentation and general experimental conditions employed have been described in detail elsewhere [9].

2.2. Electrodes and cells

An electrochemical/optical cell, constructed of Plexiglass, was used for concurrent CV, QCMB and ellipsometry experiments. The details of this cell have been presented in another paper [9]. In this cell, the working electrode (WE) consisted of an AT-cut quartz crystal (Valpey-Fisher, 5 MHz, 2.5 cm diameter), sputter-coated first with a thin film of titanium for adhesion, and then a thin film of gold. The counter electrode (CE) was a large area Pt gauze, and the reference electrode (RE) was a reversible hydrogen reference electrode (RHE).

In other experiments, a standard three-electrode, two compartment glass cell was used to electrochemically prepare and study PANI films on either a polycrystalline Pt wire (Aldrich, 99.99%, 0.5 mm diameter) WE, embedded in soft glass tubing, or a GC disc (apparent area of exposed face is ca. 0.95 cm^2) WE, embedded in an inert resin material (Scandiplast). The surface pretreatment of the Au, Pt and GC WEs prior to each experiment has been described elsewhere [10].

All potentials in this paper are reported versus the RHE and the current and charge densities are given with respect to the apparent electrode area for Au (0.45 cm^2) and GC (0.95 cm^2), and the real electrode area for Pt [11,12]. In situ ellipsometric, QCMB and CV responses were recorded simultaneously, generally using a sweep rate of 50 mV s^{-1}.

2.3. Polyaniline film growth

PANI films were grown on the gold-sputtered quartz crystals, Pt wire and GC disc WEs by cycling at 50 mV s^{-1} between 0 and ca. 1 V versus RHE in 0.1 M aniline + 1 M H_2SO_4 solution (Type I film) or between 0 and 1.7 V versus RHE in 0.02 M aniline + 1 M H_2SO_4 solution (Type II film). The PANI film thickness was estimated using the published conversion factor of 500 C cm^{-3} [9], where the anodic PANI charge is obtained from the slow sweep CVs between 0 and 0.8 V versus RHE. PANI films were removed from the Pt and Au wire electrodes by sonicating in a 30% hydrogen peroxide solution for several hours, followed by electrochemical cleaning [13]. PANI films on GC were removed by polishing, while both the PANI and underlying sputtered Au films were removed from the quartz crystals by immersion in aqua regia for ca. 24 h [13].

3. Results and discussion

3.1. General characteristics of the anodic pre-peak (A_0)

When Type I PANI films were formed at any of the three electrode substrates investigated here, the A_0 pre-peak could readily be seen in the CV scans once the films exceeded a thickness of ca. 100 nm. The solid

curve in Fig. 1(a) shows a typical CV at 50 mV s^{-1} for a 145 nm thick Type I PANI film on a GC substrate. Note that the *y*-axis is given in units of current density divided by sweep rate, in order to demonstrate the effect of sweep rate more effectively. It should be noted that slower sweep rates cause the A_0 pre-peak to attenuate and move negatively. According to the conductivity switching model [3], an increase in the sweep rate would cause the pre-peak to sharpen and shift positively, consistent with Fig. 1(a).

An important feature to note in Fig. 1(a) is the presence of a matching cathodic feature, peak C_0, to the A_0 pre-peak. Peak C_0 appears both when the upper potential limit is reversed just positive of A_0, and also when it is reversed at any potential up to 0.8 V (Fig. 1(a)). It should be noted that the cathodic C_0 feature was not predicted by the model [3] of the A_0 pre-peak arising strictly from the conversion of the PANI film from its insulating to the conducting state in the positive sweep. Indeed, the presence of peak C_0 argues that the pre-peak is likely related to the redox chemistry of some unique sites within the PANI film, perhaps in a region of lower conductivity.

When PANI films initially transform from the insulating to conducting states during an anodic sweep, it is likely that this process commences at the electrode/PANI interface [5]. Therefore, as a first hypothesis, the pre-peak may reflect the reaction of sites in this region of the film. It is not unreasonable to suggest that the binding sites of the polymer to the electrode and/or sites located near the electrode surface could be different from the sites within the bulk of the polymer film in terms of their environment, degree of hydration, or conformation. It is also possible that the metal/film interface is more resistive than the bulk of the PANI film, as was suggested in [3].

Further support for the suggestion that peaks A_0/C_0 reflect the redox activity of PANI sites near the substrate arises from the impact of the nature of the substrate on the pre-peak characteristics, when all other factors are kept constant. For example, it has been shown [10] that, for Type I PANI films, the pre-peak potential is more negative at GC versus at Au and Pt electrodes, while the principal A_1/C_1 peaks are essentially identical in nature at these three substrates. Also, the shape of the pre-peak is noticeably different

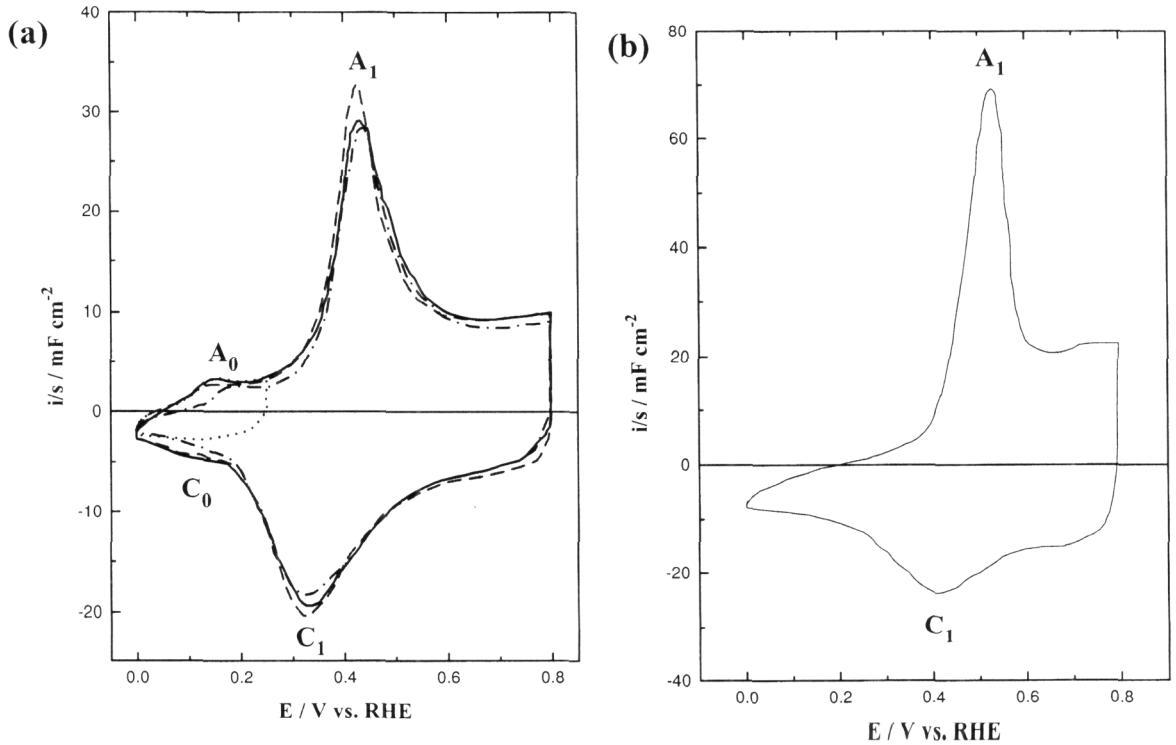

Fig. 1. An *i*/*s* plot of (a) 145 nm Type I and (b) 270 nm Type II PANI film on GC in 1 M H_2SO_4, cycled at 50 mV s^{-1} between 0 and 0.8 V (—). Also shown in (a) is the *i*/*s* response of the Type I PANI film cycled at 50 mV s^{-1} between 0 and 0.25 V (---), and at 10 mV s^{-1} (– – –) and 100 mV s^{-1} (– · –) between 0 and 0.8 V.

and its charge appears to be greatest for PANI films formed on GC, followed by Au and Pt, for otherwise the same film properties, as determined from both CV and ac impedance experiments [10].

Fig. 1(b) shows a typical CV for a Type II PANI film (270 nm), also formed on a GC substrate. Notably, both the A_0 and C_0 features are absent at this substrate, and were also never detected for a Type II film formed on Pt or Au electrodes [10]. Many attempts were made to induce these peaks to appear for Type II PANI, e.g. by increasing the film thickness, using longer cycling times, holding at negative potentials (see below), etc. but none of these were successful in yielding the anodic pre-peak. Type II films undergo the same electrochromic and conductivity switching behavior as do Type I films, and would therefore have been expected to yield the pre-peak if its origin was related to the change in the overall film conductivity. The absence of the A_0/C_0 features for Type II films again suggests that the pre-peak represents the oxidation of particular PANI sites, which would then be absent in Type II films. The observations pointed out above regarding Fig. 1a and b motivated a more careful study of the parameters affecting the pre-peak characteristics, as discussed below.

3.1.1. Effect of PANI film thickness

As Type I PANI films are grown thicker with longer potential cycling times, the pre-peak becomes easier to detect in the CV response. This dependence on film thickness may indicate that the pre-peak is associated with the onset of a fibril structure, suggested to occur at a film thickness greater than 100 nm [14,15]. However, this interpretation is inconsistent with the observation that a pre-peak is not seen for Type II films, for which the fibril structure is dominant (Fig. 2). The globular structure of Type I films (Fig. 3) is also present for thinner Type II PANI films.

Table 1 shows the charge density in the pre-peak (A_0) region, measured by using the extrapolation of the main anodic peak (A_1) as the baseline, as a function of Type I PANI film thickness on GC (using the 500 C cm^{-3} conversion factor). It is notable that the A_0 charge densities range from ca. 10 to 120 μC cm^{-2}, increasing with film thickness. This charge is generally larger than what might be expected from the one electron transfer reaction of a single monolayer of PANI. This is estimated to be ca. 20–30 μC cm^{-2}, when assuming that only every second aniline unit undergoes a one electron transfer reaction [16,17] and that full surface coverage of PANI is achieved (recalling that one monolayer of H atoms on a Pt surface is equivalent to ca. 220 μC cm^{-2} [12]). It is clear that the charge densities in Table 1 are small enough to represent a very thin layer of film.

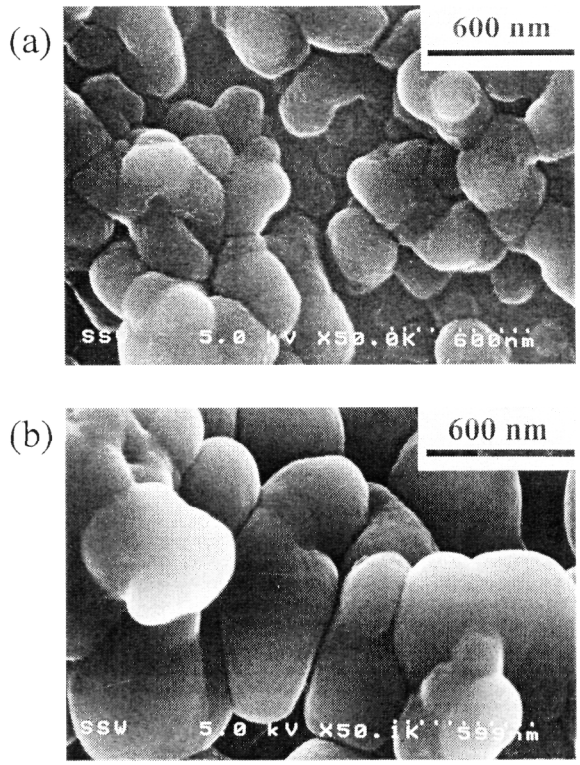

Fig. 2. FESEM view of (a) 130 nm and (b) 225 nm Type I PANI film, deposited on polycrystalline Au substrate, at a magnification of 50 000 ×, using an accelerating voltage of 5 kV. Film thickness was estimated from charge density between 0 and 0.8 V and the conversion factor of 500 C cm^{-3} of film.

It should also be pointed out that the larger size of the pre-peak with increasing PANI film thickness in Table 1 does agree with the predictions of the model proposed by Gottesfeld et al. [3]. Thicker films would have a higher film resistance and would therefore result in a greater delay in the onset of oxidation and hence a more pronounced pre-peak. The fact that no pre-peak is seen for Type II films (Fig. 1(b)), even though they are usually much thicker and hence likely to be significantly more resistive than Type I films, therefore argues for a different interfacial structure for these two types of films.

3.1.2. Effect of lower potential limit (E_-) and time at E_-

Fig. 4(a) shows that the pre-peak shifts positively and becomes sharper and larger as the potential is scanned negatively to −0.4 V for Type I PANI films on GC, consistent with the predictions of the conductivity switching model [3]. At Pt and Au, at which potentials more negative than 0 V cannot be reached due to interference from the hydrogen evolution reaction [10,11], holding the potential at 0 V for various lengths

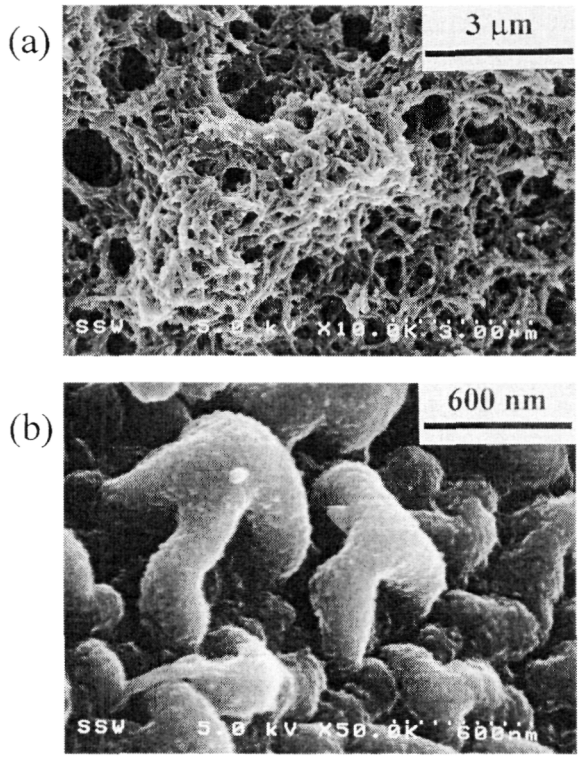

Fig. 3. FESEM view of (a) 130 nm and (b) 225 nm Type II PANI film, deposited on polycrystalline Au substrate, at two different magnifications: (a) 10 000 × and (b) 50 000 ×, respectively, using an accelerating voltage of 5 kV. Film thickness was estimated from charge density between 0 and 0.8 V and the conversion factor of 500 C cm^{-3} of film.

of times shows a similar effect as seen in Fig. 4(a). Similar experiments with Type II films still did not yield a pre-peak (Fig. 4(b)).

The change in mass of Type I PANI films at a Au substrate was tracked using simultaneous in situ QCMB, CV and ellipsometry experiments, designed to provide further information regarding changes in the film properties in relation to the anodic pre-peak. Fig. 5 shows that, after 5 min of holding at 0 V, the film mass has increased by 0.02 μg or 0.4% of its total mass (curve 2 vs. 1). In the subsequent full cycle of potential, a further mass gain is seen (curve 3 vs. 2, Fig. 5), after which the PANI film maintained a constant mass. Parallel ellipsometric measurements made as a function of time at 0 V and for a range of PANI film thickness indicated that the film refractive index, n, drops and that the film thickness increases slightly with time.

Table 1
Charge density in the pre-peak region (0–0.3 V) as a function of film thickness, determined using the 500 C cm^{-3} conversion factor, for Type I PANI films, formed on GC, in 1 M H_2SO_4

Film thickness (nm)	Charge density (μC cm^{-2})
80	10
110	45
135	75
145	120

These results indicate that, with time at negative potentials (and likely also for experiments in which E_- is extended to even more negative values), water is brought into the film, causing it to swell (consistent with the lower observed refractive index, n). As longer times at negative potentials, or more time spent at very negative potentials, cause the anodic pre-peak to shift positively, this increase in film hydration is suggested to be correlated with the anodic shift of the pre-peak. This suggests that the pre-peak potential and its shape reflect the state of hydration of PANI film sites near the metal surface. This would imply that a more positive A_0 potential indicates a higher degree, and a more negative A_0 potential, a lower extent of hydration of PANI sites deep within the film. If this is the case, perhaps Type II films, being highly porous [11] and probably containing large amounts of water, do not show the pre-peak as a separate feature, as the pre-peak potential may have been driven sufficiently positively so that it is completely submerged within the main A_1 peak.

3.2. Film annealing effects by continuous potential cycling over A_1/C_1 peaks

Another very interesting observation was made at all substrates for Type I PANI films, grown to a thickness such that the pre-peak has just appeared as a small shoulder at the foot of peak A_1. Fig. 6 shows that, for a 120 nm thick PANI film at Au, at this stage, the A_0 peak is initially rather undefined and quite positive and peak C_0 is not yet seen. After 25 min of cycling between 0 and 0.6 V (no further PANI growth), the pre-peak has moved negatively, and after a further 60 min of cycling, the C_0 peak is also clearly seen. In fact, the solid curve of Fig. 6 leaves the impression of a separate redox reaction occurring in the A_0 and C_0 peaks.

Clearly, the film properties are changing significantly with continuous potential cycling, reminiscent of the annealing effect described by Gottesfeld et al. [18]. Film annealing was suggested [18] to involve the loss of excess positive charge from the polymer backbone, leading to the expulsion of anions from the film. Consequently, neighboring PANI sites are allowed to approach closer and tighten the PANI structure and the film becomes more compact in nature. This suggested change in film properties/structure could be occurring near the Au substrate, causing the redox potential of the A_0/C_0 sites to shift negatively. As film annealing has been suggested to cause PANI to become more com-

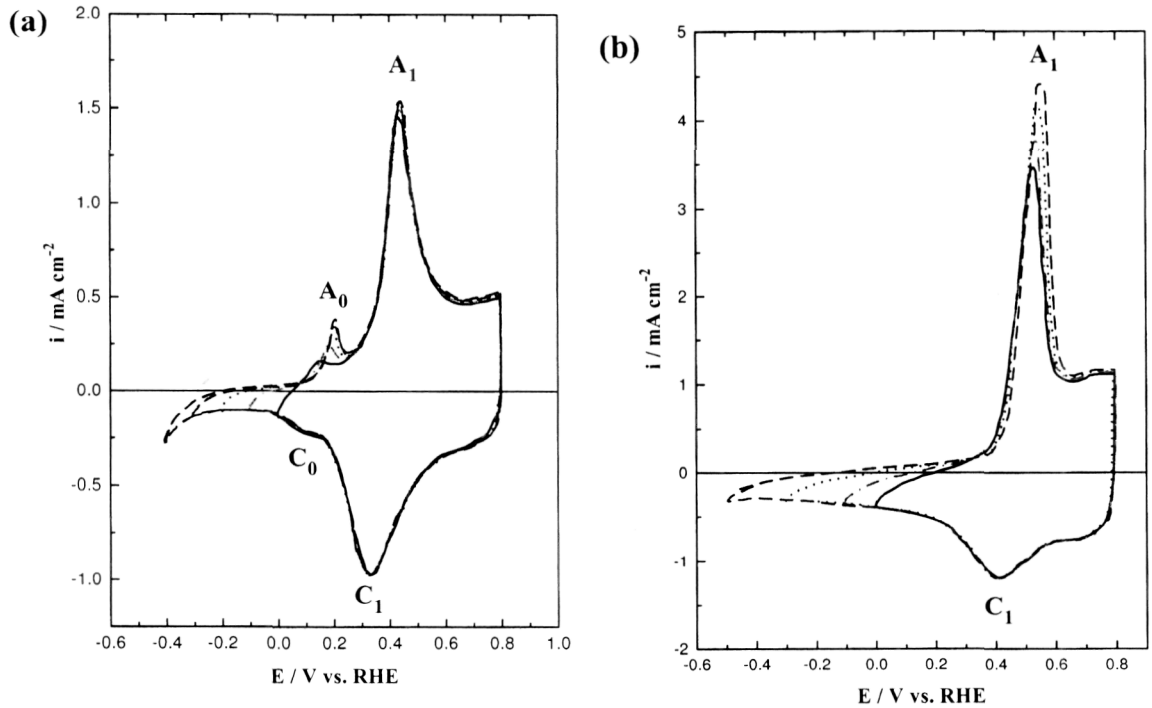

Fig. 4. The effect of the lower potential limit (E_-) on the A_0 peak for (a) 145 nm Type I and (b) 270 nm Type II PANI film, both on GC, in 1 M H_2SO_4 solution; sweep rate is 50 mV s^{-1}.

pact, containing less water, the negative shift of A_0 is completely consistent with the QCMB/A_0 peak potential results of Fig. 5.

Simultaneous ellipsometric measurements showed an increase in the extinction coefficient, k, with time of cycling, concurrent with the movement of the pre-peak to negative potentials. An increase in k indicates that PANI film is switching from a transparent, reduced form to a more absorbing material. This supports the notion of the formation of a more compact film during multi-cycling, with the negative shift in the A_0 potential serving as an indicator of this.

The mass to charge ratio during the scan through the anodic pre-peak was also calculated, both before and after the multi-cycling film annealing process was carried out. For a freshly formed PANI film, when the pre-peak is just a barely noticeable shoulder at the foot of A_1 (Fig. 6), a negligible mass change is seen during the pre-peak. This was interpreted [2] as reflecting hydrated proton expulsion and water injection during oxidation, such that the net mass change is relatively small (anions have been assumed [2,19–21] to remain uninvolved in charge compensation until potentials well into peak A_1 are reached).

However, with film annealing, and as the pre-peak moves negatively, the mass to charge ratio in the potential range of A_0 increased to as high as 7–12 g per mole of electrons. This higher mass to charge ratio may indicate that a greater amount of water is injected into the annealed film, concurrently with proton expulsion, during the anodic scan, than in the freshly formed one prior to multi-cycling. This would agree with the suggestion that the more negative A_0, the drier the internal part of the film is, thus requiring more water injection during oxidation to allow and aid ion transfer. Alternatively, the annealed film may allow the injection of anions at a much lower potential, such that the film mass increase during the scan is enhanced. A more compact film may allow film conductivity switching to occur at a lower threshold, leading to anion injection at a lower potential.

3.2.1. *Effect of anodic film degradation*

It is known that PANI films degrade when the potential is cycled above ca. 0.95 V [22–24]. Previous studies have shown that the film dissolves and other species, such as benzoquinone, are formed as a result of film degradation [1,19,23,25]. Concurrent ellipsometry, QCMB and CV experiments have been carried out to examine the nature of the PANI degradation process in more detail. PANI film degradation was carried out [9,13] by holding the potential at 1 V for various periods of time. After each period of degradation, the potential was scanned between 0 and 0.6 V until a steady-state CV was obtained, and then the ellipsometric data were collected at 0 V. A structural model of the

film was then developed to fit the ellipsometry data [9,13]. The ellipsometry analysis of Type I films during degradation shows that the inner part of the film is hardly affected in the early stages of film degradation [9]. Fig. 7 shows that interestingly, an unchanged pre-peak is still seen for such a partially degraded [2] Type I PANI film. This again supports the hypothesis that the pre-peak reflects redox activity of unique PANI sites near the substrate/polymer interface. Also, the partially degraded Type II PANI films still did not display a pre-peak, again indicating that these unique PANI sites near the substrate/polymer interface are not present in the Type II PANI films.

4. Summary

The goal of this work was to examine the A_0 pre-peak, seen for typical PANI films formed electrochemically in 1 M H_2SO_4 solution. Two types of PANI films were investigated here. Type I films are formed relatively slowly, by cycling the potential between 0 and 1 V versus RHE, as commonly done in much of the prior literature. Type II PANI films are formed by cycling the potential between 0 and 1.7 V versus RHE in 1 M H_2SO_4. These films are formed much more rapidly and are more porous than Type I films.

In the case of Type I PANI, the A_0 peak is seen for films greater than 100 nm in thickness. Often, a matching cathodic peak, C_0 is seen. The A_0/C_0 peaks are never seen for Type II films, even when they are made very thick. These results suggest that the pre-peak arises from the oxidation of particular PANI sites within the film. The notable substrate dependence of the pre-peak potential, the continuing presence of the pre-peak for a partially degraded Type I PANI film (known to degrade primarily on its outer surface) [9] and the relatively small charge density associated with the pre-peak, all suggest that peak A_0 reflects the reaction of PANI sites near the underlying substrate. This region of the film may be more resistive than the bulk of the PANI film, as suggested earlier [3].

Simultaneous CV, QCMB and ellipsometry measurements suggest that the movement of the pre-peak to positive potentials, as a result of holding at 0 V, is related to film swelling. Type II films are known to be more porous and therefore it is possible that they already contain a high quantity of water, thus having moved the A_0 pre-peak positively into the main A_1 redox peak. This would explain why the A_0 peak is never seen as a separate CV feature for Type II films.

It has been reported earlier that time of cycling of PANI films over the full range of potential from 0 to 0.6 V versus RHE causes Type I films to anneal, presumably resulting in a more compact PANI film

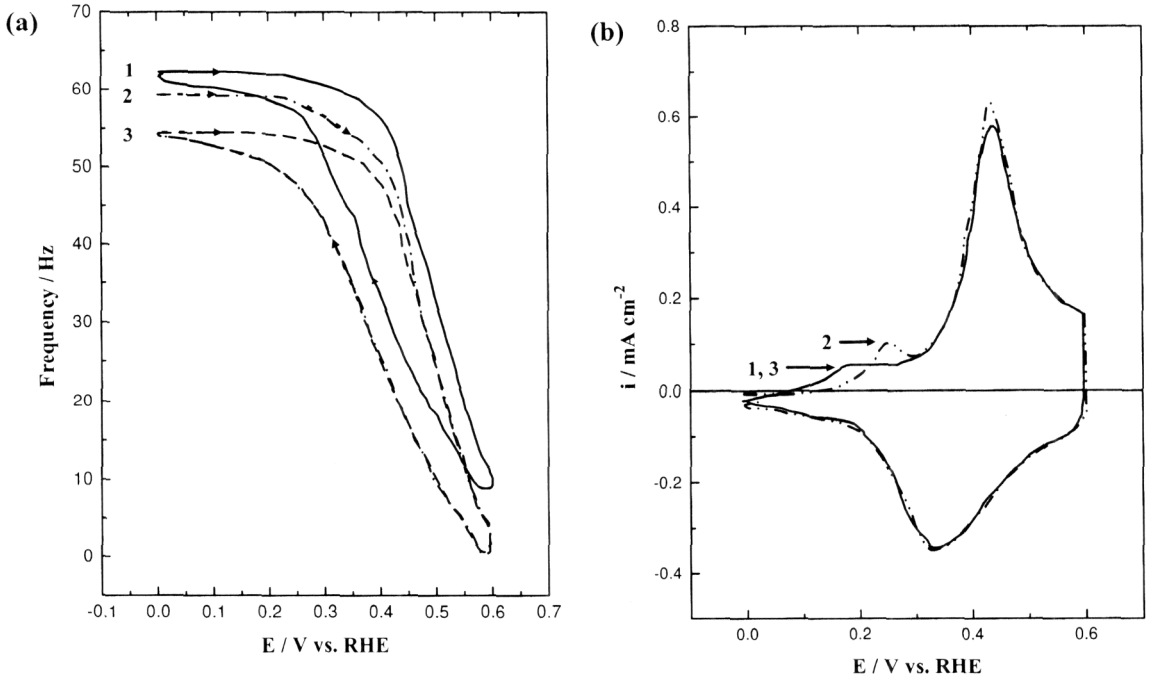

Fig. 5. The frequency–potential response (a) and the corresponding CV (b) for a 120 nm Type I PANI film deposited on a Au-sputtered quartz crystal substrate; (1) when the potential is first scanned between 0 and 0.6 V (—) at 20 mV s^{-1} in 1 M H_2SO_4. The potential was then held at 0 V for 5 min, showing a decrease in frequency from 1 to 2, followed by a scan to 0.6 V (– - –) and then (3) subsequent multi-scans between 0 and 0.6 V (---).

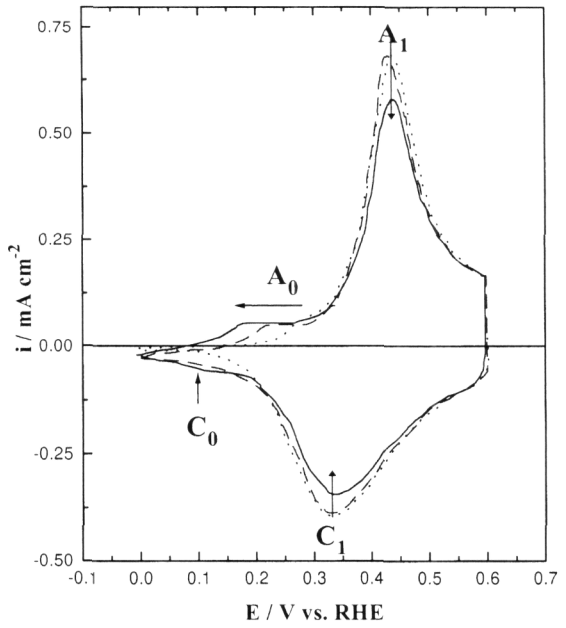

Fig. 6. CV response for a 120 nm Type I PANI film, deposited on a Au-sputtered quartz crystal substrate, as a function of time of cycling between 0 and 0.6 V at 20 mV s^{-1}: (a) 0 (---); (b) 25 (– – –) and (c) 85 min (—).

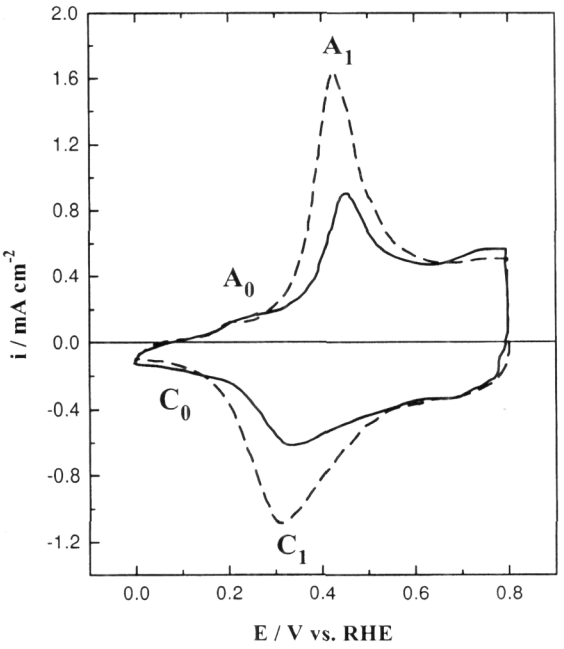

Fig. 7. CV response for a 110 nm, partially (30%) degraded (—) Type I PANI film, initially 145 nm thick (– – –), on GC. The film was degraded by cycling between −0.3 and 1.2 V versus RHE at 50 mV s^{-1} in 1 M H_2SO_4 solution.

[18]. Film annealing carried out in this way is shown here to be accompanied by a gradual negative shift of the pre-peak. This is consistent with our QCMB and ellipsometry results described above, as the negative shift of peak A_0 would then reflect a lower film water content. Notably, even very long times of cycling of Type II films does not reveal a pre-peak, which would have been expected to emerge from peak A_1 and move negatively.

Simultaneous QCMB experiments show that the film mass per mole of electrons, determined for the pre-peak region, increases with time of film annealing. It is possible that more water is being injected upon film oxidation to facilitate ion transport because film annealing causes the internal part of the film to be drier. It is also possible that more solution anions are being injected during the oxidation of the pre-peak sites.

Acknowledgements

The authors are grateful to the Natural Sciences and Engineering Research Council of Canada (NSERC) for their overall support of this work. H.N. Dinh also acknowledges scholarship support from NSERC, IODE, Alberta Heritage Foundation, A.S.M. International Calgary Chapter, and the University of Calgary. The authors also wish to thank Dr M. Wagter of Surface Science Western for the FESEM analysis.

References

[1] A. Redondo, E.A. Ticianelli, S. Gottesfeld, Mol. Cryst. Liq. Cryst. 160 (1988) 185.
[2] H.N. Dinh, V.I. Birss, J. Electroanal. Chem. 443 (1998) 63.
[3] S. Gottesfeld, A. Redondo, I. Rubinstein, S.W. Feldberg, J. Electroanal. Chem. 265 (1989) 15.
[4] S. Gottesfeld, A. Redondo, S.W. Feldberg, J. Electrochem. Soc. 134 (1987) 271.
[5] M. Kalaji, L.M. Peter, L.M. Abrantes, J.C. Mesquita, J. Electroanal. Chem. 274 (1989) 289.
[6] V.I. Birss, C. Bock, H. Elzanowska, Can. J. Chem. 75 (1997) 1687.
[7] B.E. Conway, J. Mozota, Electrochim. Acta 28 (1983) 9.
[8] H. Elzanowska, V.I. Birss, J. Appl. Electrochem. 23 (1993) 646.
[9] H.N. Dinh, J. Ding, S.J. Xia, V.I. Birss, J. Electroanal. Chem. (in press).
[10] H.N. Dinh, V.I. Birss, J. Electrochem. Soc. (in preparation).
[11] H.N. Dinh, P. Vanýsek, V.I. Birss, J. Electrochem. Soc. (in preparation).
[12] M. Breither, J. Electroanal. Chem. 90 (1978) 425.
[13] H.N. Dinh, Ph.D. Dissertation, The University of Calgary, September 1998.
[14] C.M.G.S. Cruz, E.A. Ticianelli, J. Electroanal. Chem. 428 (1997) 185.
[15] K. Bade, V. Tsakova, J.W. Schultze, Electrochim. Acta 37 (1992) 2255.

[16] W.-S. Huang, B.D. Humphrey, A.G. MacDiarmid, J. Chem. Soc. Faraday Trans. I 82 (1986) 2385.
[17] P.M. McManus, R.J. Cushman, S.C. Yang, J. Phys. Chem. 91 (1987) 744.
[18] E. Sabatani, A. Redondo, J. Rishpon, A. Rudge, I. Rubinstein, S. Gottesfeld, J. Chem. Soc. Faradary Trans. 89 (1993) 287.
[19] D. Orata, D.A. Buttry, J. Am. Chem. Soc. 109 (1987) 3574.
[20] R.M. Torresi, S.I. Cordoba de Torresi, C. Gabrielli, M. Keddam, H. Takenouti, Synth. Met. 61 (1993) 291.
[21] C. Barbero, M.C. Miras, O. Haas, R. Kötz, J. Electrochem. Soc. 138 (1991) 669.
[22] T. Kobayashi, H. Yoneyama, H. Tamura, J. Electroanal. Chem. 177 (1984) 293.
[23] D.E. Stilwell, S.-M. Park, J. Electrochem. Soc. 135 (1988) 2491.
[24] A.Q. Zhang, C.Q. Cui, J.Y. Lee, Synth. Met. 72 (1995) 217.
[25] D.E. Stilwell, S.-M. Park, J Electrochem. Soc. 135 (1988) 2497.